Polarization charges and polarization-induced barriers in $Al_xGa_{1-x}N$/GaN and $In_yGa_{1-y}N$/GaN heterostructures

L. Jia,[a] E. T. Yu, D. Keogh, and P. M. Asbeck
Department of Electrical and Computer Engineering, University of California, San Diego, La Jolla, California 92093-0407

P. Miraglia, A. Roskowski, and R. F. Davis
Department of Materials Science and Engineering, North Carolina State University, Raleigh, North Carolina 27695-7907

(Received 14 June 2001; accepted for publication 14 August 2001)

Polarization charges are measured and the formation of large electrostatic barriers arising primarily as a consequence of the presence of polarization-induced charge densities is deduced from capacitance–voltage analysis of n-type $Al_xGa_{1-x}N$/GaN and $In_yGa_{1-y}N$/GaN heterostructures. In structures consisting of 5–10 nm $Al_xGa_{1-x}N$ or $In_yGa_{1-y}N$ surrounded by n-GaN, capacitance–voltage profiling studies combined with elementary electrostatic analysis yield experimental estimates of polarization charge densities, which are compared with values expected based on the combined effects of spontaneous and piezoelectric polarization. These results imply the existence of electrostatic barriers that are due primarily to the large polarization charge densities at each heterojunction interface and the resulting potential difference maintained across the thin $Al_xGa_{1-x}N$ or $In_yGa_{1-y}N$ layers. The electrostatic barriers formed in these structures are large in comparison to the heterojunction conduction-band offsets, demonstrating the utility of polarization-based engineering of electrostatic barriers in nitride semiconductor heterostructures. © *2001 American Institute of Physics.* [DOI: 10.1063/1.1412594]

There has been intense interest and research activity in recent years directed towards the application of III–V nitride materials in high-power, microwave-frequency electronic devices. Much of this effort has focused on the development of $Al_xGa_{1-x}N$/GaN heterostructure field-effect transistors (HFETs), with outstanding progress in dc and microwave performance having been made by a number of groups.[1–5] Vertical nitride-based device structures such as heterojunction bipolar transistors (HBTs) are of interest as well,[6] although development of high-performance HBTs will most likely require further improvements in p-type GaN conductivity and fabrication of low-resistance ohmic contacts to p-GaN. Spontaneous and piezoelectric polarization effects in the nitrides make possible a variety of new approaches in the engineering of both bipolar and unipolar vertical nitride device structures, based on the engineering of electrostatic potentials and carrier distributions via the judicious, deliberate placement of polarization charge densities within a heterostructure.

In this letter, we describe the design, fabrication, and characterization of $Al_xGa_{1-x}N$/GaN and $In_yGa_{1-y}N$/GaN heterostructures in which polarization effects are exploited to create a large electrostatic barrier within each heterostructure. A related approach has been used previously to increase the peak barrier height in $Al_xGa_{1-x}N$/GaN HFETs.[7,8] Our studies yield values for polarization charge densities in good agreement with those expected from the combined effects of spontaneous and piezoelectric polarization for $Al_xGa_{1-x}N$/GaN interfaces, but somewhat lower than expected for $In_yGa_{1-y}N$/GaN. In addition, our results strongly imply the existence of large, polarization-induced barriers within each heterostructure. For a 10 nm $Al_{0.13}Ga_{0.87}N$ layer surrounded by n-GaN, the polarization-induced component of the barrier height is estimated to be over 1 eV, demonstrating that polarization charges at nitride semiconductor heterojunction interfaces are a highly effective tool for use in engineering of large electrostatic barriers in nitride heterostructure devices.

Samples for this study were grown by metalorganic chemical vapor deposition (MOCVD) on conducting 6H SiC substrates. Trimethylaluminum, triethylgallium, and trimethylindium were employed as group III precursors and purified ammonia as a group V precursor. A 100 nm high temperature AlN buffer layer and a 500 nm n^+-GaN contact layer were deposited initially for each sample at 1100 and 1020 °C, respectively. Subsequent layers consisted of 150–200 nm GaN doped using silane to a Si concentration of 2×10^{17} cm^{-3} followed by a thin, nominally undoped $Al_xGa_{1-x}N$ or $In_yGa_{1-y}N$ layer, and finally a GaN cap layer 120–200 nm in thickness, also Si doped at a concentration of 2×10^{17} cm^{-3}. The MOCVD-grown layers all had Ga-terminated surfaces. Three samples were studied, containing a 5 nm $Al_{0.13}Ga_{0.87}N$ layer, a 10 nm $Al_{0.13}Ga_{0.87}N$ layer (each deposited at 1020 °C), and a 5 nm $In_{0.08}Ga_{0.92}N$ layer deposited at 780 °C, respectively. Circular Schottky contacts 130 μm in diameter were formed by deposition of 100 nm Ni. Ohmic contacts formed on the sample surfaces consisted of annealed Al/Ti metallization. Schematic diagrams of representative sample structures and the corresponding band-edge energy profiles and charge densities are shown in Fig. 1.

In the $Al_xGa_{1-x}N$/GaN structures, the presence of the

[a]Electronic mail: ljia@ece.ucsd.edu

Downloaded 10 Nov 2001 to 132.239.19.110. Redistribution subject to AIP license or copyright, see http://ojps.aip.org/aplo/aplcr.jsp

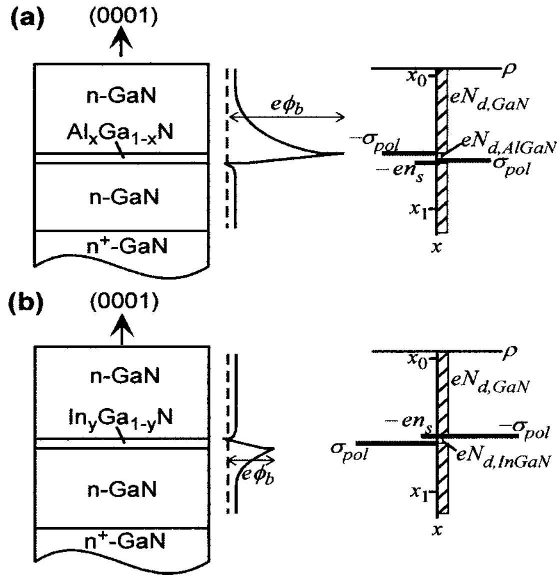

FIG. 1. Schematic diagrams of the epitaxial layer structure, energy-band-edge profile, and electrostatic charge density for (a) an $Al_xGa_{1-x}N$/GaN single-barrier heterostructure and (b) an $In_yGa_{1-y}N$/GaN single-barrier heterostructure. Note that $\sigma_{pol}<0$ for the $In_yGa_{1-y}N$/GaN structure.

polarization dipoles with surface charges σ_{pol} and $-\sigma_{pol}$ at the lower and upper $Al_xGa_{1-x}N$/GaN heterointerfaces, respectively, produces a potential change ϕ_{pol}, given by $\sigma_{pol}d/\epsilon_{AlGaN}$, where d is the thickness of the $Al_xGa_{1-x}N$ layer and ϵ_{AlGaN} is its dielectric constant. This potential change results in the existence of a peak in potential energy of height $e\phi_b$, whose value is modified from $e\phi_{pol}$ by the effects of the induced compensating charges and by the conduction-band offset energy associated with the heterojunctions. The value of ϕ_b can be obtained approximately by solution of the following equations corresponding to the charge neutrality condition and integration of Poisson's equation, respectively:

$$eN_{d,\mathrm{GaN}}\sqrt{2\epsilon_{\mathrm{GaN}}(\phi_b-\Delta E_c/e-E_{f,\mathrm{GaN}}/e)/eN_{d,\mathrm{GaN}}} + eN_{d,\mathrm{AlGaN}}d-en_s=0, \quad (1)$$

$$\phi_b=\phi_{\mathrm{pol}}-en_s d/\epsilon_{\mathrm{AlGaN}}+eN_{d,\mathrm{AlGaN}}d^2/2\epsilon_{\mathrm{AlGaN}}+(\Delta E_c - E_{f,hj})/e, \quad (2)$$

where e is the electronic charge, ϵ_{GaN} is the dielectric constant of GaN, $N_{d,GaN}$ and $N_{d,AlGaN}$ are the donor concentrations in the upper GaN layer and in the $Al_xGa_{1-x}N$ layer, respectively, ΔE_c is the $Al_xGa_{1-x}N$/GaN conduction-band offset, $E_{f,GaN}$ is the Fermi level within the upper GaN layer, $E_{f,hj}$ is the Fermi level at the lower $Al_xGa_{1-x}N$/GaN interface, and n_s is the electron sheet concentration at that interface. A similar analysis may be employed to derive ϕ_{pol} and ϕ_b for the $In_yGa_{1-y}N$/GaN heterostructure.

Capacitance–voltage ($C-V$) profiling was used to determine the charge and electrostatic potential distributions in these samples. Apparent carrier concentration profiles $\hat{n}(x)$ can be obtained from measured $C-V$ profiles according to the relationship

$$\hat{n}(x)=\frac{2}{e\epsilon}\left(\frac{d}{dV}\frac{1}{C^2}\right)^{-1}, \quad x=\epsilon/C. \quad (3)$$

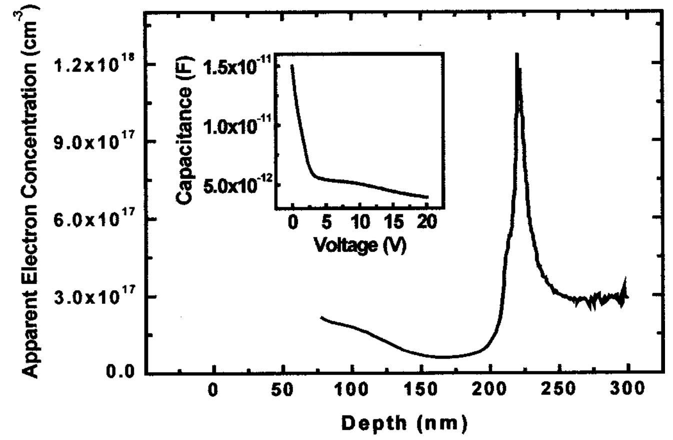

FIG. 2. Apparent carrier concentration profile for sample 1, derived from $C-V$ profiling data (inset).

The $C-V$ profile and corresponding carrier concentration profile are shown for samples 1 and 3 in Figs. 2 and 3, respectively. The electrostatic potential $\phi(x)$ within each device structure must satisfy[9,10]

$$\phi(x_1)-\phi(x_0)=\int_{x_0}^{x_1}\frac{1}{\epsilon}[eN_d(x)+\rho_{\mathrm{pol}}(x)-en(x)]x\,dx = \int_{x_0}^{x_1}\frac{1}{\epsilon}[eN_d(x)+\rho_{\mathrm{pol}}(x)-e\hat{n}(x)]x\,dx, \quad (4)$$

where $N_d(x)$ is the donor concentration profile, $\rho_{pol}(x)$ the polarization charge density profile, and $n(x)$ the true electron concentration profile in the device. As shown in Figure 1, x_0 and x_1 are points in the GaN layers at which the electric field associated with the presence of the $Al_xGa_{1-x}N$ or $In_yGa_{1-y}N$ layer has vanished. Given the dopant concentrations and apparent carrier concentration profiles derived from $C-V$ measurements as shown in Fig. 2, the polarization-induced potential change ϕ_{pol} can then be obtained from Eq. (4), and is found to be given by

$$\phi_{\mathrm{pol}}=\int_{x_0}^{x_1}\frac{1}{\epsilon}\rho_{\mathrm{pol}}(x)x\,dx=-\int_{x_0}^{x_1}\frac{e}{\epsilon}[N_d(x)-\hat{n}(x)]x\,dx. \quad (5)$$

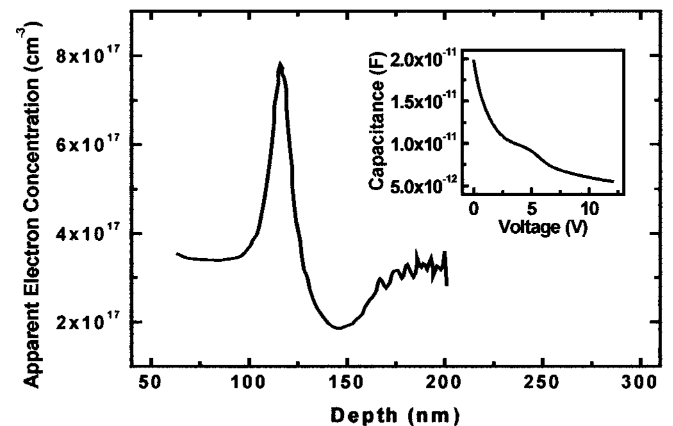

FIG. 3. Apparent carrier concentration profile for sample 3, derived from $C-V$ profiling data (inset).

Downloaded 10 Nov 2001 to 132.239.19.110. Redistribution subject to AIP license or copyright, see http://ojps.aip.org/aplo/aplcr.jsp

TABLE I. Layer thickness and composition of $Al_xGa_{1-x}N/GaN$ and $In_yGa_{1-y}N/GaN$ single-barrier heterostructures. Experimentally determined values for polarization charge density and polarization-induced barrier height are also shown. For comparison, the expected values for polarization-induced barrier height are listed.

Sample No.	Barrier layer	$\sigma_{pol}(\times 10^{12}\ e/cm^2)$ measured	ϕ_{pol} (eV) measured	ϕ_{pol} (eV) expected
1	10 nm $Al_{0.13}Ga_{0.87}N$	7.24±0.04	1.31±0.01	1.50
2	5 nm $Al_{0.13}Ga_{0.87}N$	7.1 ±0.1	0.64±0.01	0.75
3	5 nm $In_{0.08}Ga_{0.92}N$	4.1 ±0.1	0.36±0.01	0.99

The barrier height ϕ_b can then be obtained by solution of Eqs. (1) and (2). Alternatively, n_s can be determined directly by integrating the apparent carrier concentration profile in the vicinity of the lower $Al_xGa_{1-x}N/GaN$ interface or the upper $In_yGa_{1-y}N/GaN$ interface. ϕ_b can then be computed using Eq. (2).

It is interesting to note that the value of ϕ_{pol} is not strongly sensitive to the detailed distribution of the group III elements within the barrier. For example, if the aluminum mole fraction in the $Al_xGa_{1-x}N$ has a distribution $a(x)$, then there will be a polarization distribution $P(x)\sim Ka(x)$ and an associated charge density distribution $\rho_{pol}(x)=-dP/dx\sim -K\ da(x)/dx$ where K corresponds to an effective piezoelectric coefficient, assumed to be constant over the range of variation of $a(x)$. Then the effective polarization barrier ϕ_{pol} is given by $\int(1/\epsilon)\rho_{pol}(x)x\,dx=-(K/\epsilon)\int[da(x)/dx]x\,dx$ computed across the barrier. Integrating by parts shows that $\phi_{pol}=(K/\epsilon)\int a(x)dx$, which depends only on the total amount of aluminum incorporated in the structure. In our analysis, we assume that the aluminum distribution in the $Al_xGa_{1-x}N$ is uniform, so the polarization barrier ϕ_{pol} becomes $\int(1/\epsilon)\rho_{pol}(x)x\,dx=\sigma_{pol}d/\epsilon_{AlGaN}$, as mentioned above.

Applying the former analysis to the three samples studied, we obtain values for the polarization charge in each sample as shown in Table I. The polarization charge densities for the $Al_xGa_{1-x}N/GaN$ samples are in good agreement with expected values: using available values[11] for spontaneous polarization, piezoelectric coefficients, and elastic constants, a polarization charge density of magnitude $8.3\times 10^{12}\ e/cm^2$ is expected to be present at the $Al_{0.13}Ga_{0.87}N/GaN$ heterojunction interface, compared to values of 7.2×10^{12} and $7.1\times 10^{12}\ e/cm^2$ derived from our measurements for samples 1 and 2, respectively. For the $In_{0.08}Ga_{0.92}N/GaN$ sample, a polarization charge density of $4.1\times 10^{12}\ e/cm^2$ is derived, somewhat lower than the expected value of $1.1\times 10^{13}\ e/cm^2$. This discrepancy is of uncertain origin, and may arise from uncertainties in the $In_yGa_{1-y}N$ composition, layer thickness, spontaneous polarization, or piezoelectric coefficient, or from charged defects in the InGaN layer.

The polarization-induced potential change ϕ_{pol}, calculated according to Eq. (5), is shown for each sample in Table I. Our measurements yield 1.3 and 0.6 eV for ϕ_{pol} for samples 1 and 2, respectively; these compare well with the theoretically expected values of 1.5 and 0.75 eV. For sample 3, the experimentally determined value of ϕ_{pol} is somewhat lower than that expected theoretically. The values obtained for ϕ_{pol} in samples 1 and 2 are particularly interesting given that the conduction-band offset for the $Al_{0.13}Ga_{0.87}N/GaN$ heterojunction is estimated to be approximately $\Delta E_c=0.26$ eV: most of the total barrier height in these structures arises from the presence of the polarization charges at the heterojunction interfaces rather than from the conduction-band offsets. Indeed, these results demonstrate that polarization charges in thin III–V nitride layers are a powerful tool for engineering of electrostatic barriers in nitride heterostructure devices.

Our analysis also provides insight into the factors that exert the most pronounced influence on the design of such barrier structures. For $Al_xGa_{1-x}N/GaN$ heterostructures, the polarization charge increases in rough proportion to the Al concentration in the $Al_xGa_{1-x}N$ layer; increased Al concentration is therefore the most effective approach for increasing the barrier height for the structure shown in Fig. 1(a). An increase in the $Al_xGa_{1-x}N$ layer thickness can also be highly effective, since the change in electrostatic potential associated with the polarization charge increases directly with the $Al_xGa_{1-x}N$ layer thickness. Analogous behavior is expected for the $In_yGa_{1-y}N/GaN$ structure shown in Fig. 1(b).

In summary, we have performed $C-V$ characterization and analysis of $Al_xGa_{1-x}N/GaN$ and $In_yGa_{1-y}N/GaN$ single-barrier heterostructures. Our studies provide estimates of polarization charges present at each heterojunction interface, and demonstrate that large electrostatic barriers can be formed within a nitride heterostructure largely as a consequence of the spontaneous and piezoelectric polarization charges present at these interfaces. The barriers arising due to the presence of polarization charges can be several times larger than those due to the band offsets at the nitride heterojunction interface, demonstrating the utility of polarization effects as tools for engineering of electrostatic barriers in nitride heterostructures.

One of the authors (L. J.) would like to thank D. Qiao, E. Miller, and Professor S. S. Lau for their useful discussions. Part of this work was supported by the ONR POLARIS MURI program (Dr. Colin Wood).

[1] Y. F. Wu, B. P. Keller, P. Fini, S. Keller, T. J. Jenkins, L. T. Kehias, S. P. DenBaars, and U. K. Mishra, IEEE Electron Device Lett. **19**, 50 (1998).
[2] S. T. Sheppard, K. Doverspike, W. L. Pribble, S. T. Allen, J. W. Palmour, L. T. Kehias, and T. J. Jenkins, IEEE Electron Device Lett. **20**, 161 (1999).
[3] G. J. Sullivan, M. Y. Chen, J. A. Higgins, J. W. Yang, Q. Chen, R. L. Pierson, and B. T. McDermott, IEEE Electron Device Lett. **19**, 198 (1998).
[4] N. X. Nguyen, M. Micovic, W. S. Wong, P. Hashimoto, L. M. McCray, P. Janke, and C. Nguyen, Electron. Lett. **36**, 468 (2000).
[5] Q. Chen, R. Gaska, M. Asif Khan, M. S. Shur, A. Ping, I. Adesida, J. Burm, W. J. Schaff, and L. F. Eastman, Electron. Lett. **33**, 637 (1997).
[6] L. S. McCarthy, P. Kozodoy, M. J. W. Rodwell, S. P. DenBaars, and U. K. Mishra, IEEE Electron Device Lett. **20**, 277 (1999).
[7] E. T. Yu, X. Z. Dang, L. S. Yu, D. Qiao, P. M. Asbeck, S. S. Lau, G. J. Sullivan, K. S. Boutros, and J. M. Redwing, Appl. Phys. Lett. **73**, 1880 (1998).
[8] X. Z. Dang, R. J. Welty, D. Qiao, P. M. Asbeck, S. S. Lau, E. T. Yu, K. S. Boutros, and J. M. Redwing, Electron. Lett. **35**, 602 (1999).
[9] H. Kroemer, W.-Y. Chien, J. S. Harris, Jr., and D. D. Edwall, Appl. Phys. Lett. **36**, 295 (1980).
[10] H. Kroemer, Appl. Phys. Lett. **46**, 504 (1985).
[11] E. T. Yu, P. M. Asbeck, S. S. Lau, X. Z. Dang, and G. J. Sullivan, J. Vac. Sci. Technol. B **17**, 1742 (1999).

Downloaded 10 Nov 2001 to 132.239.19.110. Redistribution subject to AIP license or copyright, see http://ojps.aip.org/aplo/aplcr.jsp